

New Gasostatic Borehole Bearings – Construction and Research

Franciszek ORYŃSKI

*Higher Vocational State School in Włocławek
3. Maja 17, 87–800 Włocławek, Poland*

Witold PAWŁOWSKI

*Institute of Machine Tools and Production Engineering
Lodz University of Technology
Stefanowskiego 1/15, 90-924 Łódź, Poland*

Sławomir KAWCZYŃSKI

*Faculty of Technical Sciences
Cuiavian University in Włocławek
Freedom Square 1, 87–800 Włocławek, Poland*

Received (20 December 2015)

Revised (16 January 2016)

Accepted (11 February 2016)

In the article the origin of creation, construction as well as the research of the novel gasostatic borehole bearings are presented. In the first part of the paper the information on the construction of the bearing is outlined whereas in the second part the methodology of the experimental and numerical research as well as obtained results are described. The paper is summarized with the conclusions of the research and suggestions due to commercial application of the bearings.

Keywords: Aerostatic bearings, bearings systems, gas compressor bearings.

1. Introduction

Contemporarily applied bearing systems include different types of bearings. The most popular one is roller system based on the very well developed ball and roller bearings. However, application of roller systems shows some drawbacks. In the case of high velocities the required accuracy of the bearing elements results in high cost of the manufacturing, which often exceeds the acceptable level of expenses. In the case of high load capacity the overall dimensions as well as the mass of the bearings rise problems in their mechanical applications [12]. The abovementioned problems give rise to increasing interest in other types of bearing i.e. oil, gas or magnetic bearings [14]. Application of those types of bearings is also limited. In the case of gas

bearings the load is significantly limited. In the case of oil or magnetic bearings the special power supply systems are required. However, their common advantage is low overall dimension and high level of rotation speed. The manufacturing technologies which are involved in their production are not as sophisticated as the ones required in case of roller bearings.

In the compressors installed in Polish section of the Yamal gas pipeline the hydrodynamic bearing are applied. The additional oil supplying systems for those bearings as well as the oil–gas separating devices are required. It results in high cost of purchase and maintenance of the bearing systems. Having analyzed pros and cons of the bearing being hitherto applied [1], the different solution has been undertaken to be examined in which the compressed gas is the bearing medium. This scientific problem is the scope of research which included design of the bearing system prototype which could prove that application of high–pressurized gas as the bearing medium can provide sufficient load of the bearing system [4]. The ultimate goal of the research is to exchange the hydrodynamic bearing system into gas bearing system applied in the gas compression stations of the pipeline system.

2. Construction of the gas bearings

In the aerostatic bearing systems the compressed air from external source is connected to the chamber through the inlet orifice (damper). Subsequently, the gas flows from the chamber to the outlet slot, which results in gradual decreasing the pressure rate down to the atmospheric pressure. The gas medium under pressure provides force which balances external load and prevents from direct contact of the both surfaces of the bearing. Thus working conditions remain in the range of fluid friction. In order to supply the medium to the bearing, the special guides are machined in the bushing. The guides are usually applied in the form of holes, chambers and distribution grooves. Dimensions of the guides are supposed to be small in order to avoid the self–induced vibrations [13]. Due to small dimension of the bearing guides and chambers, the technological problems can arise and special tools have to be applied.

Having analyzed the available publications in that field, the new type of bearing has been designed: gasostatic borehole bearings. The research of radial–axial serial bearing system as well as radial bearing system with damping on load surfaces were carried out.

The gasostatic borehole radial–axial serial bearing with internal damping [5] is presented in Fig. 1. The bearing is equipped with the bushing 1 with small radial holes (eight holes in two rows – 2 and 3). The bushing surrounds the pin 4. Between the bushing and the pin there are three cylindrical slots 5, 6 and 7. The middle one 5 is bigger than the other two slots 6 and 7. On both sides of the bushing 1 there are vertical discs 8 and 9 mounted on the pin in order to bear axial loads. Between the discs 8 and 9 and the bushing there are two front slots on each sides (10 and 11, 12 and 13) and the inner slots 10 and 12 are bigger than the outer ones 11 and 13. The dimensions of the slots were derived experimentally by comparing load capacity of the bearing for different slot sizes.

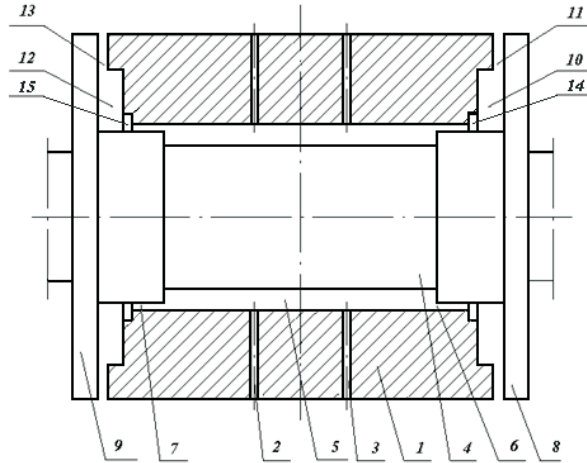


Figure 1 The radial-axial bearing scheme [5]

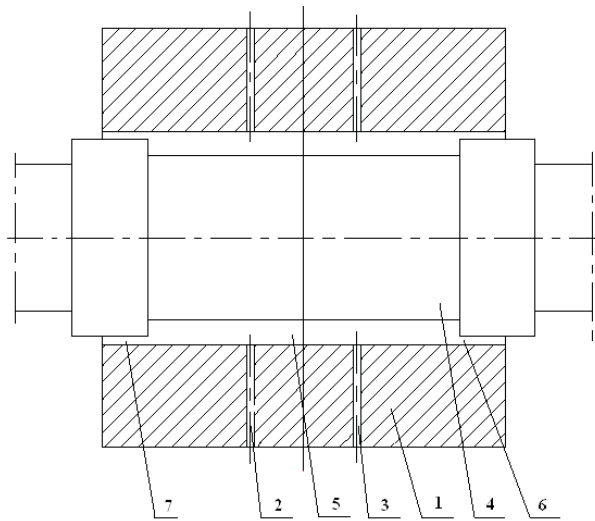


Figure 2 The radial bearing scheme [6]

Between radial and axial bearing there are two undercuts 14 and 15, which create the pressure equalizing spaces around the pin for the radial bearing. It provides even distribution of the gas pressure entering the axial bearing.

The construction of the radial bearing presented in Fig. 2 [6] is similar to the radial-axial bearing. The radial bearing is not equipped with vertical discs on both sides of the bushing.

3. Principle of operation of the gas bearings

The principle of operation and pressure distribution of the radial-axial serial gas borehole bearing [5] is illustrated in Fig. 3. The gas medium is delivered under equal pressure to all holes in two rows 2 and 3 of the bushing 1 (Fig. 1). Flowing through the holes of small diameter the gas is damped down to the pressure p_z . In the case of idle working (without load) it flows around pin 4 under the same pressure p_z between rows 2 and 3. Subsequently the gas flows on in both directions firstly along the radial slot 5, then along smaller slots 6 and 7. Then the gas flows radially along front slots 10 and 11 or 12 and 13. Pressure of the gas is gradually decreasing. The smaller slot, the bigger pressure gradient. In the case of no load the pressure distribution along the pin and discs is symmetrical. The pressure in the radial bearing decreases from p_z down to p_w on the edge of the radial part of the bearing. The p_w is the equalized pressure in the undercuts 14 and 15. In the axial bearing the pressure decreases according to the presented characteristics from p_w down to p_n in the outlet of the bearing. Two rows of the holes 2 and 3 as well as the discs mounted on the pin 4, the bearing is not susceptible to skew along the longitudinal axis.

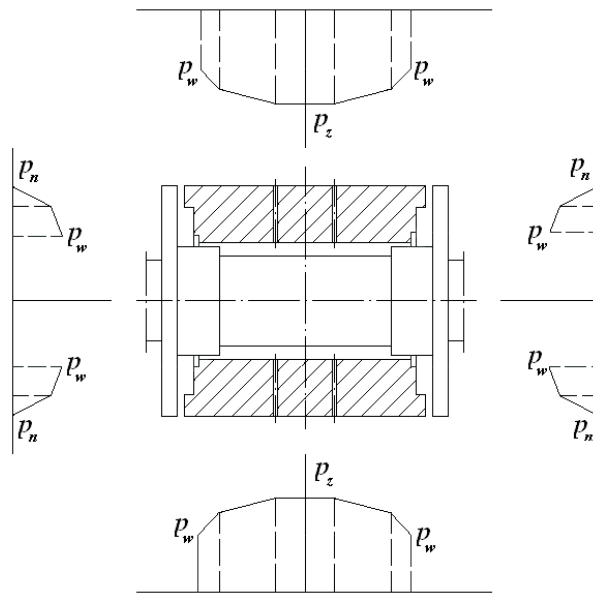


Figure 3 The pressure distribution of the unloaded bearing

After loading the pin 4 with shear lateral force it starts to move perpendicularly to the axis. It results in changing the dimension of cylindrical slots. Decreasing size of the slots results in pressure growth and respectively increasing size of the slots results in pressure drop. The pressure difference creates the force counteracting the lateral load of the bearing. After loading the pin 4 with axial force the front slots

change their dimensions and the pressure difference on both sides of the bushing 1 counteracts the axial load of the bearing.

As shown in Fig. 2 the radial bearing works similarly. The only difference is that pressure of the gas flowing along the axis decreases from p_z down to p_n . The principle of the load counteracting force creation as well as response to any disruption is similar to the radial part of the abovementioned radial-axial serial bearing.

4. Experimental research of the gas bearings system

The diagram of the test stand of the gas bearings system is presented in Fig. 4. The stand contains examined bearing system consisting of the radial-axial bearing (1, 2) and radial bearing (3, 4). The main shaft is driven by means of three-phase asynchronous motor 17 connected with the flexible coupling 18. The rotational speed of the shaft is controlled by the inverter. The shear forces are excited pneumatically by two nozzles 10 and 11 mounted on both sides of the bearings system. Pressure of the excitation is indicated with two manometers 13 and 14. The displacement of the shaft is measured with position sensor 15 by OMRON (ZX-EM02T) in the middle between the bearings. The sensor is equipped with the indicator of the current position 16 resolution of which is 0.001 mm.

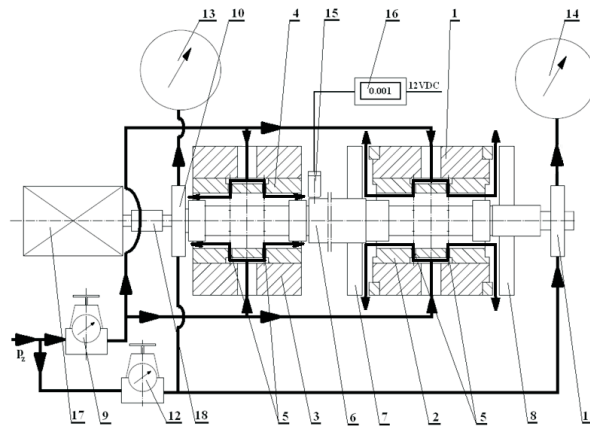


Figure 4 The experimental test stand of the bearings system

1 - body of the radial-axial bearing, 2 - bushing of the radial-axial bearing, 3 - body of the radial bearing, 4 - bushing of the radial bearing, 5 - holes of gas supply, 6 - shaft, 7, 8 - discs of the radial-axial bearing, 9 - gas supply regulator, 10, 11 - nozzles of the load system, 12 - load regulator, 13, 14 - manometers, 15 - shaft displacement sensors, 16 - indicator of shaft displacement, 17 - motor, 18 - clutch

Experimental tests were performed at different supply pressures (0.70 MPa and 0.80 MPa), rotational speeds of the shaft (0 min^{-1} , 1700 min^{-1} , 2350 min^{-1} and 2900 min^{-1}) and load force. The measurements were repeated three times and the results were averaged (Fig. 5 and Fig. 6).

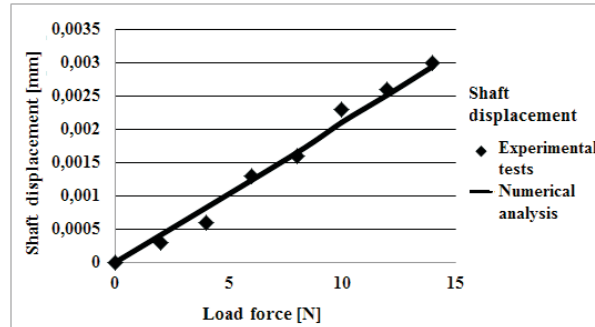


Figure 5 Results of experimental tests and numerical analysis of the shaft displacement versus load force for rotation speed of the shaft of 2900 min^{-1} and supply pressure 0.70 MPa

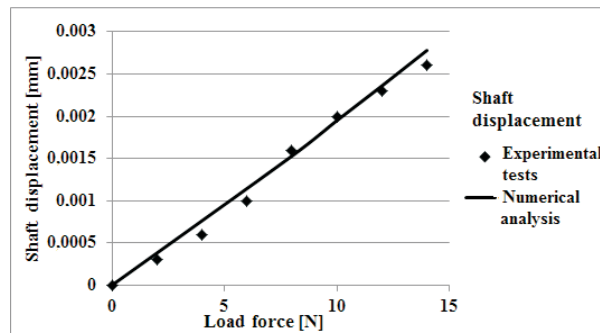


Figure 6 Results of experimental tests and numerical analysis of the shaft displacement versus load force for rotation speed of the shaft of 2900 min^{-1} and supply pressure 0.80 MPa

The experiments of the bearing system prototype were performed in order to check application capacities of the design idea of the gasostatic borehole bearings system and show the basic properties of the examined system. Having analyzed results of abovementioned research it can be considered that rigidity of the whole tested system in the perpendicular direction is ca. $0,2 \mu\text{m}/\text{N}$. The minimal radial dimension of the slot (interspace) of the bearing is $30 \mu\text{m}$, therefore the maximum load force should not exceed 150 N to avoid contact of the bushing and the pin surface. The maximum load of 150 N is obtained experimentally for this test prototype which size is ca. five times smaller than that of target real application e.g. gas compressors bearing system.

Moreover, obtained results show very slight effect of supply pressure on the shaft displacement for selected values of supply pressures. The effect of rotational speed on the shaft displacement is also very low.

5. Numerical analyses

The next stage of the research was creating bearing simulation program in Matlab – Simulink environment. The mathematical equations of Newton's second law and mass conservation law were used [11]. Bearing space was divided into parts (chambers) and gas flow equations were written for it.

The dynamics of motion of the cylindrical bearing shaft (journal) is described with the following equations [11]:

$$\begin{aligned} m \frac{d^2 y}{dt^2} &= - \sum_{i=1}^k \left[F p_i \cos \alpha_i + T_i \sin \alpha_i + T_{i,i+1} \sin \left(\alpha_i + \frac{\pi}{k} \right) \right] + P_y(t) m \frac{d^2 z}{dt^2} \\ &= - \sum_{i=1}^k \left[F p_i \sin \alpha_i + T_i \cos \alpha_i + T_{i,i+1} \cos \left(\alpha_i + \frac{\pi}{k} \right) \right] + P_z(t) m \frac{d^2 x}{dt^2} \\ &= - \sum_{i=1}^k F_i p_i + P_x(t) \end{aligned}$$

where: m – mass of the shaft reduced to a central point; x, y, z – moving the shaft relative to the x, y, z axis; P_x, P_y, P_z – loading force components, i – the number of chambers, k – number of chambers in one row in the bearing, F – the chamber surface, p_i – pressure in the i^{th} chamber, α_i – chamber position angle, T_i – tangential friction force in the area of the angle α_i , $T_{i,i+1}$ – tangential friction force in the area of the angle $\alpha_{i,i+1}$

The mass flow rate for the different parts of the bearing can be derived from the general form of the following equation [2, 3]:

$$\sum Q_i = F \dot{w}_i \frac{p_i}{p_N} + \frac{V_i}{p_N} \dot{p}_i$$

where: $\sum Q_i$ – flow rate of the gas supplied to and discharged from the i^{th} chamber, w_i – journal movement perpendicular to the i^{th} chamber resulting from the external load, V_i – volume of the i^{th} chamber, p_N – normal pressure

On the basis of the equations of dynamics and flow rates of the axial and radial-axial bearing system the functional model of that system was created in Matlab–Simulink software.

The input geometrical and mass parameters as well as results of the analyses based on the mathematical formulae [2, 3] are summarized as follows:

- Mass of the shaft 7 kg
- Length of the shaft 0.604 m
- Bearing spacing 0.396 m

The analysis of the shaft displacement versus load force was performed in order to check the model behavior and to compare the model response and experimental tests results. Shaft displacement analysis was performed for the same physical parameters like at the workstation and the results are shown in the graphs (Fig. 5 and Fig. 6).

The results obtained in numerical simulation (Fig. 5 and Fig. 6) are highly convergent to the results of the experimental tests of the shaft displacement versus load force.

Having successfully checked the results convergence of experimental and theoretical rigidity tests, the basic dynamic properties of the analyzed system were derived analytically by means of that Matlab–Simulink model. The results of the dynamic analyses (run-up/run-out tests) based on the mathematical formulae are summarized as follows:

- Maximal amplitude of the shaft vibration $1.5 \mu\text{m}$
- Frequency of the shaft for cylindrical form of movement 150.46 Hz
- Frequency of the shaft for conical form of movement 241.36 Hz
- Maximal frequency of the shaft rotation 50 Hz.

The analytical results presented above indicate clearly that the working point of the system is far beneath the first resonance frequency and the whole system works in subcritical conditions.

6. Conclusions

The numerical and experimental tests of the gasostatic bearing system can be summarized as follows:

1. The load capacity of the new bearing system is sufficient to sustain rotational movement of the shaft loaded with certain range of forces.
2. Analytically derived value of first mode frequency (150.46 Hz) is much higher than that of operational rotational speed of the shaft (50 Hz).
3. The maximal amplitude obtained during numerical analyses ($1.5 \mu\text{m}$) is far lower than the bearing interspace ($30 \mu\text{m}$), which indicates that the bearing can work safely.

Application of the gasostatic borehole bearings with internal damping can be competitive alternative for hitherto used gas or hydraulic bearings. Ease of construction and technology as well as small overall dimensions of the bearings are undisputed advantages especially for application in high-speed rotational mechanisms e.g. gas compressors of the pipelines. Low cost of the bearings production is the other aspect which can bring about significant economic effect.

The gasostatic bearings of different construction variants are the subjects of patent applications [5–10].

References

- [1] Demierre, J., Rubino, A. and Jürg Schiffmann, J.: Modeling and Experimental Investigation of an Oil-Free Microcompressor–Turbine Unit for an Organic Rankine Cycle Driven Heat Pump, *Journal of Engineering for Gas Turbines and Power*, Paper No: GTP-14-1364; doi: 10.1115/1.4028389.

- [2] **Lewandowski, D.:** Aerostatic bearing of high-speed spindle systems (in Polish), *Scientific Papers of Technical University of Lodz*, No 753, Łódź, Poland, **1996**.
- [3] **Oryński, F.:** Design and calculation of hydraulic friction vibration damper with the contactless piston and automatic quick-acting choke (in Polish), *Hydraulics and Pneumatics*, No 3, 14 – 17.
- [4] **Oryński, F. and Kawczyński, S.:** The choice of bearings for gas compressors (in Polish), *Hydraulics and Pneumatics*, No 6, 14 – 19.
- [5] **Oryński, F. and Kawczyński, S.:** Gasostatic radial – axial borehole bearing [with undercuts on the shaft and bearings foreheads]. Zgłoszenie patentowe P398005, *Polish patent application*, 06.02.2012.
- [6] **Oryński, F. and Kawczyński, S.:** Gasostatic radial borehole bearing [with undercuts on the shaft]. The patent application P-398003, *Polish patent application*, 06.02.2012.
- [7] **Oryński, F. and Kawczyński, S.:** Gasostatic radial borehole bearing [with undercuts on bearing foreheads]. The patent application P398004, *Polish patent application*, 06.02.2012.
- [8] **Oryński, F. and Kawczyński, S.:** Gasostatic radial – axial borehole bearing [with undercuts on the shaft and discs]. The patent application P398006, *Polish patent application*, 06.02.2012
- [9] **Oryński, F. and Kawczyński, S.:** Gasostatic radial – axial borehole bearing [with undercuts on bushing and foreheads]. The patent application P398007, *Polish patent application*, 06.02.2012.
- [10] **Oryński, F. and Kawczyński, S.:** Gasostatic radial – axial borehole bearing [with undercuts on bushing and discs]. The patent application P398008, *Polish patent application*, 06.02.2012.
- [11] **Oryński, F. and Pawłowski, W.:** The mathematical description of dynamics of the cylindrical grinder, *International Journal of Machine Tools and Manufacture*, No. 42/7, 773–780.
- [12] **Oryński, F. and Pawłowski, W.:** Simulation and Experimental Research of the Grinder's Wheelhead Dynamics, *Journal of Vibration and Control*, vol. 10, No. 6, 915–930.
- [13] **Pawłowski, W.:** Dynamic Model of Oscillation-Assisted Cylindrical Plunge Grinding With Chatter, *Journal of Manufacturing Science and Engineering*, 135(5):051010-051010-6, doi:10.1115/1.4024819.
- [14] **Wade, J. L., Lubell, D. R. and Weissert, D.:** Successful Oil-Free Version of a Gas Compressor Through Integrated Design of Foil Bearings, *ASME Proceedings*, Vol. 5: Structures and Dynamics, No. GT2008-50349, doi:10.1115/GT2008-50349, 969–973.

